Int. J. Heat Mass Transfer. Vol. 27, No. 1, pp. 113–123, 1984
Printed in Great Britain

0017–9310/84 $3.00 + 0.00

MELTING AND SOLIDIFICATION OF A METAL SYSTEM IN A RECTANGULAR CAVITY

C. GAU and R. VISKANTA
School of Mechanical Engineering, Purdue University, West Lafayette, IN 47907, U.S.A.

(*Received* 23 *February* 1983 *and in revised form* 16 *May* 1983)

Abstract—The role of natural convection on solid–liquid interface motion during melting and solidification of Lipowitz metal in a rectangular cavity was studied. The measurements of both temperature distributions and temperature fluctuations were used as a qualitative indication of the natural convection flow regimes and structures of melt during phase transformation. The measured and predicted solid–liquid interface positions during solidification from below and above, as well as melting from above and below, show reasonably good correspondence. The suppression of natural convection in the Lipowitz metal, which is not taken into account in the model, leads to a slower rate of melting and a higher rate of freezing than that predicted.

NOMENCLATURE

c	specific heat
Fo	Fourier number, $\alpha t/H^2$
g	gravitational acceleration
H	height of the cavity
Δh_f	Latent heat of fusion of the phase change material
h	heat transfer coefficient
k	thermal conductivity
k^*	thermal conductivity ratio, k_l/k_s
Nu	Nusselt number, $h(1-\delta)H/k_l$
Pr	Prandtl number, ν/α_l
Ra	Rayleigh number, $g\beta(T_{wb}-T_f)(H-s)^3/\nu\alpha_l$
Ste_l	Stefan number, $c_l(T_w-T_f)/\Delta h_f$
Ste_s	Stefan number, $c_s(T_f-T_{wt})/\Delta h_f$
s	solid–liquid interface position
T	temperature
W	width of the cavity
x	horizontal distance from the central symmetric line
y	vertical distance from the top of the cavity
z	horizontal distance normal to the x–y plane.

Greek symbols

α	thermal diffusivity
β	thermal expansion coefficient of liquid
ρ	density
ν	kinematic viscosity
τ	$Fo\,Ste$; $\tau_l = Fo_l\,Ste_l$ and $\tau_s = Fo_s\,Ste_s$
θ	dimensionless temperature, $(T-T_{wt})/(T_f-T_{wt})$
ξ	dimensionless distance, y/H
δ	dimensionless interface position, s/H.

Subscripts

b	bottom plate
f	fusion point of PCM
l	liquid state
0	initial state
s	solid state
t	top plate
w	wall.

1. INTRODUCTION

SOLID–LIQUID phase-change heat transfer involving melting and solidification has received considerable attention and an up-to-date review of the literature is available [1]. Most of the work done in the past, however, has used relatively high Prandtl number fluids such as paraffins and water as test materials; and natural convection has been shown either to enhance the melting rate or to retard the freezing rate [2]. Phase-change heat transfer concerned with natural convection in metals, on the other hand, has received relatively little attention, although these materials are of particular interest in metallurgy, materials processing and crystal growth [3].

A usual assumption in analyzing phase-change heat transfer in a metal system is that conduction is the sole mode of energy transfer because metals have high thermal conductivity [4]. Natural convection in the melt during solidification of metals has also received much attention because of its role in modifying the solid structure [5]. Especially in the manufacturing of semiconductors and castings, experiments have shown that the structure and distribution of inclusions in the solid is significantly affected by the buoyancy-induced flow in the melt during solidification [6]. Cole and Winegard [7] have shown that the amount of thermal convection during a horizontal and unidirectional solidification is a function of the temperature gradient in the liquid, the rate of solidification, the height of the solid–liquid interface, the angle of deviation of the interface from the vertical plane, and the fluid parameters of the liquid metal. Furthermore, the analysis of experiments [8] involving a cylindrical column of lead during downward freezing showed that heat transfer rates associated with Bénard convection are less under transient than under steady-state conditions.

The study of natural convection effects on the solidification and melting processes in metals has received little attention. Szekely and Chhabra [9] were the first to demonstrate, experimentally and analytically, the effect of natural convection on the shape of a stationary and a transient interface in a

rectangular tank with a heat source and sink on the two vertical sidewalls.

The objective of this paper is to report on the effect of natural convection on the solid–liquid interface motion during melting and solidification of a metal in a cavity. The importance of natural convection in the melt will be demonstrated from the measurements of temperature distributions and temperature fluctuations. The flow patterns will be deduced indirectly, and the measured solid–liquid interface positions will be compared with predictions based on an analytical model.

2. EXPERIMENTS

2.1. *Apparatus and instrumentation*

Solidification and melting experiments were performed in a rectangular test cell (Fig. 1) that had inside dimensions of 8.89 cm in height, 6.35 cm in width, and 3.81 cm in depth. The two horizontal walls, which served as the heat source/sink, were made of a multipass heat exchanger machined out of copper plate. The copper surfaces were plated with a layer of 0.0127 mm thick chromium for protection against corrosion. All of the vertical walls were made of Lexan (polycarbonate resin): the two vertical sidewalls were 1.27 cm thick plates of Lexan to support the cell; and, for better insulation, the front and back walls had a 0.318 cm air gap between the plates. One of the plates was 0.318 cm thick and the other was 0.635 cm thick. All the joints between the Lexan plates were sealed with vacuum grease.

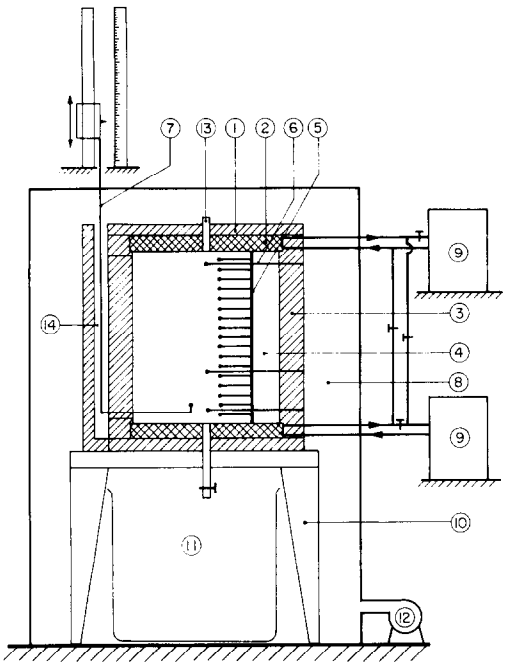

FIG. 1. Schematic diagram of test apparatus: (1) insulation, (2) heat exchanger, (3) Lexan wall, (4) phase change material, (5) thermocouple rack, (6) small diameter thermocouples, (7) L-shaped movable probe, (8) temperature controlled environment, (9) constant temperature bath, (10) support frame, (11) container, (12) heat gun with temperature controller, (13) hole for inserting movable probe, (14) vertical slot.

Five thermocouples were inserted through the copper plates and epoxyed separately into five small diameter holes drilled close to the surface of the copper plates. A vertical slot 0.159 cm in width by 7.62 cm in length was milled in one of the vertical sidewalls for the insertion of an L-shaped probe. Through the vertical slot the liquid PCM could be sucked in or expelled by the contraction or expansion of PCM during phase transformation. A 0.635 cm diameter hole, drilled through the bottom plate and connected with a tube coupled with the vertical slot in the sidewall, served to drain the liquid and to expose the shape of the solid–liquid interface. To prevent the freezing of the material in the tube at the bottom of the cell and on the outside of the vertical slot, a long narrow diameter cable electric heater was immersed and heated.

Eighteen calibrated thermocouples (with an accuracy of $\pm 0.1°C$) each having a wire diameter of 0.127 mm and sheathed in a 1.27 mm O.D. stainless steel tube, were spaced equally in the center of the test cell to measure the temperature distributions. The beads of the thermocouples were coated with a thin layer of epoxy for protection. The thermocouple rack could be removed when not in use.

Three thermocouples each with a wire diameter of 0.0762 mm were installed in the frame of the thermocouple rack. One was located near the bottom and a second near the top. The last thermocouple was placed near the middle of the cell for measuring the temperature fluctuations. The junctions were coated with a thin layer of high thermal conductivity epoxy. The DC part of the signal of the temperature fluctuations was suppressed by an adjustable DC suppressor so that the small AC component could be amplified and recorded.

To measure the temperature fluctuations when the thermocouple rack was not in use, three additional thermocouples were inserted through three small holes drilled separately on the vertical wall that had no slot. The first was located in the central region at a position 4.67 mm above the bottom plate, the second and third were positioned 24 and 77.79 mm, respectively, above the bottom plate. The beads were also coated with a thin layer of high thermal conductivity epoxy for protection. The holes were then sealed with silicon glue.

The test cell was placed in a transparent box made of Lexan where the temperature could be regulated and kept constant by a temperature controller. The purpose of the controlled environment was to reduce the temperature difference between the test cell and to minimize the heat loss/gain from the test cell to the ambient surroundings. A heat storage material was also placed in the box to minimize the frequent on-and-off switching of the heater and to keep the inside temperature close to a constant value.

2.2. *Experimental procedure and data reduction*

In experiments the working material used was Lipowitz eutectic (commercial name: Cerrobend) with a composition of: Bi, 50%; Pb, 26.7%; Sn, 13.3%; Cd, 10%; and a melting temperature of 70°C. The thermophysical properties are summarized in Table 1. The thermal conductivity and the viscosity of the liquid could not be found in the literature; therefore, properties given for an alloy system of similar composition (Bi, 50.3%; Pb, 31.2%; Sn, 8.8%; Cd, 9.7%) were used. The thermal conductivity of the liquid in the temperature range 70–100°C was given as 5.489 $W\,m^{-1}\,K^{-1}$ and the kinematic viscosity at a temperature of 106°C as $0.331 \times 10^{-6}\,m^2\,s^{-1}$ [11]. The Lipowitz eutectic was chosen because of the ease of handling and the reasonable cost.

Before each experiment the solid Cerrobend was melted and poured into the preheated test cell through the sprue on the LHS. Provision was made to avoid air bubble entrapment in the test cell. This was accomplished during the filling procedure by a slight lifting of one of the side walls where a small hole had been drilled near the top plate. This hole was sealed after the test cell was filled.

The initial temperature inside the test cell was kept uniform and only a single phase was allowed to exist. This was done by circulating a constant temperature fluid in both heat exchangers at a temperature slightly above or below the fusion point for a sufficient period of time. Melting or solidification was initiated by switching one of the heat exchangers to another constant temperature bath preset at a different temperature. A uniform solid temperature was reached, usually between 1–2°C below the fusion temperature of the eutectic, before melting was initiated. This was done to eliminate the subcooling as a parameter of the problem.

Both the pour-out method and the probing method were used to examine and/or measure the shape of the solid–liquid interface. In the pour-out method, the liquid was poured out at a predetermined time through the sprue or through the tube at the bottom of the cell. The interface was exposed and examined. In the probing method, a Vernier caliper was used to measure the distance the probe traversed in the liquid. In the melting experiments from above and the freezing experiments from below, a glass rod was used as a probe and inserted in the test cell through a hole drilled in the central region of the top plate. In the melting experiments from below and the freezing experiments from above, where the hole in the top plate was blocked by the solid, an L-shaped probe was used and inserted in the liquid region through the sprue. This L-shaped probe allowed for a vertical motion along the vertical slot milled in the sidewall between the sprue and the test cell. The measurement error resulting from the deflection of the probe tip during the measuring period was predetermined and minimized.

Table 1. Thermophysical properties of Lipowitz eutectic (Bi, 50%; Pb, 26.7%; Sn, 13.3%; Cd, 10% [10])

	Solid	Liquid
ρ [$kg\,m^{-3}$]	9400	9400
c [$kJ\,kg^{-1}\,K^{-1}$]	0.167	0.167
k [$W\,m^{-1}\,K^{-1}$]	19.0	5.499
ν [$m^2\,s^{-1}$]		0.331×10^{-6}
Δh_f [$kJ\,kg^{-1}$]	32.6	
T_f [°C]	70.0	
β [$°C^{-1}$]		6.6×10^{-5}
Pr (based on $k = 7.68\,W\,m^{-1}\,K^{-1}$)		6.76×10^{-2}

3. ANALYSIS

Before beginning the analysis and experiments using the probing method, the experiment using the pour-out method was performed to examine the shape of the solid–liquid interface. It was found during melting and freezing that the solid–liquid interface at the positions observed was flat or nearly flat. This finding justifies the assumption of one-dimensional (1-D) freezing and melting in the analysis for the boundary conditions imposed. The observations, therefore, have encouraged the use of a simple 1-D model to predict the solid–liquid interface motion instead of solving the complete system of three-dimensional (3-D) momentum and energy equations with a moving boundary.

We assume that all of the thermophysical properties, except the density in the buoyancy term, are constant. The rate of melting (freezing) is controlled by the relative magnitude of the heat transfer to each side of the solid–liquid interface and the latent heat of fusion absorbed (liberated) at the interface. Lacking a better data base, natural convection heat transfer in the liquid at the interface was modeled by steady heat transfer correlations for cavities without phase change.

The nonlinearity introduced by the motion of the solid–liquid interface and natural convection in the liquid precluded a closed form analytical solution of the model equations. Therefore, among the different techniques available for solving the problem [1], the integral method was adopted because of its simplicity.

In dimensionless form, the energy balance at the interface ($\xi = \delta$) becomes

$$\frac{d\delta}{d\tau_s} = \frac{\partial\theta}{\partial\xi} + k^* \frac{Nu}{(1-\delta)}(\theta_{wb} - 1). \tag{1}$$

The energy equation in the solid can be expressed as

$$Ste_s \frac{\partial\theta_s}{\partial\tau_s} = \frac{\partial^2\theta}{\partial\xi^2}. \tag{2}$$

The initial, boundary, and interface conditions become, respectively

$$\theta_1 = \theta_0 \geqslant 1, \quad \delta = 0, \quad \tau_s \leqslant \text{during freezing}, \tag{3}$$

$$\theta_s = \theta_0 \leqslant 1, \quad \delta = 1, \quad \tau_s \leqslant \text{during melting}, \tag{4}$$

$$\theta_s = 0, \quad \xi = 0, \tag{5}$$

$$\theta_l = \theta_{wb}, \xi = 1, \quad (6)$$

$$\theta_l = \theta_s = 1, \xi = \delta. \quad (7)$$

We assume a second-order polynomial in ξ for the temperature distribution

$$\theta = \phi(\tau_s)(\xi/\delta) + [1-\phi(\tau_s)](\xi/\delta)^2, \quad (8)$$

which satisfies the temperature boundary conditions. The unknown function $\phi(\tau_s)$ can be found by the following procedure. Differentiation of equation (7) with respect to time, τ_s, at $\xi = \delta$ yields

$$\frac{\partial\theta_s}{\partial\xi}\cdot\frac{\partial\delta}{\partial\tau_s} + \frac{\partial\theta}{\partial\tau_s} = 0. \quad (9)$$

We eliminate $d\delta/d\tau_s$ and $d\theta_s/d\tau_s$ by combining it with equations (1) and (2) to obtain the necessary condition to determine $\phi(\tau_s)$

$$\left[Ste_s\left[\frac{\partial\theta_s}{\partial\xi}\right]\left[\frac{\partial\theta_s}{\partial\xi} + k^*\frac{Nu}{(1-\delta)}(\theta_{wb}-1) + \frac{\partial^2\theta_s}{\partial\xi^2}\right]_{\xi=\delta}\right] = 0. \quad (10)$$

Substituting equation (8) into equation (10) and solving, yields

$$2-\phi = |-(b+c)+\sqrt{[(b+c)^2+4c]}|/2, \quad (11)$$

where

$$b = \left[\frac{\delta}{1-\delta}\right]k^* Nu(\theta_{wb}-1); \quad c = 2/Ste_s.$$

The final form of the differential equation for the position of the solid–liquid interface becomes

$$\frac{d\delta}{d\tau_s} = \left[\frac{2-\phi}{\delta}\right] + k^*\frac{Nu}{(1-\delta)}[\theta_{wb}-1]. \quad (12)$$

This equation can be solved numerically for the interface position δ. The Nusselt number correlations for the natural convective heat transfer coefficients needed in the model equations, equations (11) and (12), were taken from ref. [12].

The results for freezing show that the solid–liquid positions are not sensitive to the change in the Stefan numbers when they are less or close to 0.1, which is within the range obtained in the experimental conditions for the material used. However, the motion of the solid–liquid interface is affected by the superheating of the liquid, especially when natural convection is present. This can retard and eventually terminate the motion of the solid–liquid interface.

For melting, the only parameter affecting the motion of the solid–liquid interface is the Stefan number. The larger the Stefan number, the steeper the slope of the curve for the interface position. At later times during the melting process, natural convection becomes turbulent, and the melt layer thickness increases linearly with dimensionless time τ_l.

4. RESULTS AND DISCUSSION

4.1. *Freezing from below and melting from above*

4.1.1. *Comparison of measured and predicted interface positions.* In the experiments of freezing from below and melting from above, the temperatures measured did not show any oscillations or fluctuations throughout the entire phase transformation process. However, the initiation of fluid motion or natural convection (if it existed) and the motion of the solid–liquid interface imply that the flow in the liquid is unsteady. Therefore, the temperatures measured at the two locations which are not affected by the coupling between the flow and the temperature fields and the transient nature of the phenomenon suggest that the fluid is stagnant. Natural convection does not occur during phase transformation for these configurations, and heat conduction is the sole mode of energy transfer in the liquid.

Figure 2 shows the comparison of the measured and predicted interface positions for melting from above. Data for the thermal conductivity of liquid Lipowitz metal was not found in the literature. In experiments under the same thermal driving force (the same temperature difference between the boundary and the

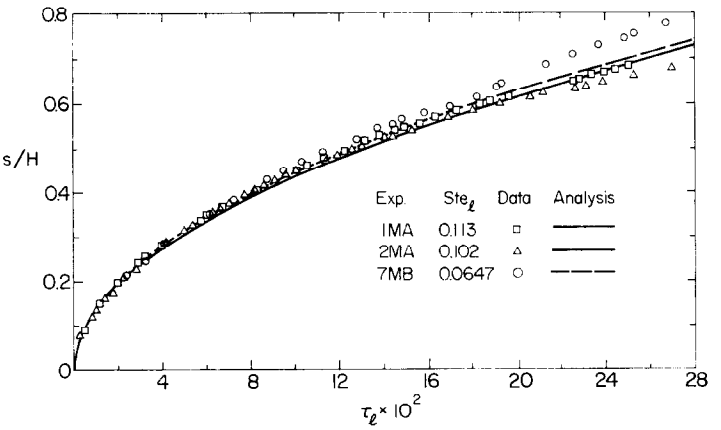

FIG. 2. Comparison of predicted and measured solid–liquid interface positions for melting from above.

interface during melting and freezing), the observed melting rates much lower than the freezing rates suggest that the thermal conductivity of the liquid Lipowitz metal is lower than for the solid. Therefore, the conductivity data for a metal with a similar composition (Bi, 50.3%; Pb, 31.2%; Sn, 8.8%; Cd, 9.7%) found in ref. [10] (see Table 1) was used. Unfortunately, the thermal conductivity of alloys is quite sensitive to their composition. The experimental data for the interface position was found to fall above the predicted one. It was therefore decided to adjust the thermal conductivity of the liquid by comparing the predictions with the experimental data for Lipowitz metal. Good agreement was obtained (Fig. 2) when the thermal conductivity of the liquid was increased by a factor of 1.4 from the value given in Table 1. The value of 7.68 W m^{-1} K^{-1} was used for the thermal conductivity of liquid Lipowitz metal for the results reported in this paper.

A comparison of measured and predicted interface positions during solidification is shown in Fig. 3. In general, good agreement is obtained. The experimental data for the motion of the freezing front are initially below and later above the predicted ones. The initial slower solidification rate is attributed in some degree to the probe which retarded the growth of the solid in the measured region. It took approximately 5–10 s to measure the position of the solid–liquid interface. If the probe could measure the position of the interface at the same place each time, a significant measurement error would result. During the solidification process at later times the temperature measured in the liquid indicated a supercooling of approximately 2°C. The dendrites at the interface may have grown during this time and may have accelerated the solidification rate. This characteristic was also observed in freezing of another system [13].

4.2. *Melting from below*

4.2.1. *Temperature distributions.* Before initiating the melting experiments the temperature distribution of the solid was set uniform and close to the fusion temperature. In the early stages of melting ($t \leqslant 40$ min), the temperature profile (Fig. 4) in the liquid layer appears to be linear. Apparently laminar natural convection in metal is insufficiently intense to produce a non-linear temperature distribution. Conduction is the predominant mode of heat transfer. Even during the transition from laminar to turbulent flow (as indicated by the increased frequency and amplitude of temperature oscillations in Fig. 5) in the time interval between $t = 40$ and 68 min, the temperature distribution is still linear (Fig. 4). After the melt has reached a certain depth or the correspondingly critical Rayleigh number has been exceeded, the temperature distribution in the liquid layer changes drastically. This is attributed to a complete change in the flow structure. The temperature fluctuation measurements indicate a random oscillation of temperature. The flow at this stage is considered to be turbulent (well mixed) due to the ascent and descent of thermals. An isothermal turbulent core which results from the effective mixing of the melt can be inferred from Fig. 4 for $t \geqslant 70$ min. Thermal boundary layers which have steep temperature gradients near the bottom plate and the solid–liquid interface have formed. These findings are similar to those for the melting of paraffin from below [14]. As expected, however, the thermal boundary layers in the metal system (low Prandtl number fluid) appear to be thicker than in the paraffin system (high Prandtl fluid).

4.2.2. *Temperature fluctuations.* Temperature fluctuations were measured at different locations in the cell and the results suggest different flow regimes. Therefore, for the sake of clarity, the measurements are discussed separately for the laminar, transition and turbulent regimes, and when natural convection is suppressed in the liquid.

The temperature fluctuations measured with the thermocouple located in the central region near the bottom plate are shown in Fig. 5. During the initial

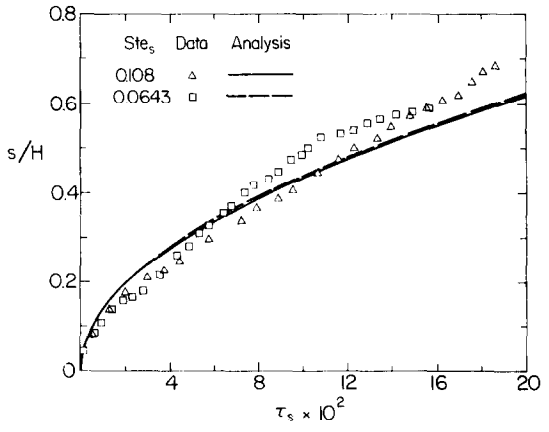

FIG. 3. Comparison of predicted and measured solid–liquid interface positions for freezing from below.

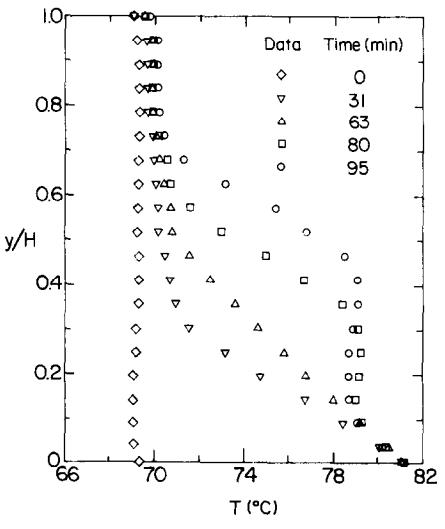

FIG. 4. Temperature distribution during melting from below with $T_{wb} = 81.1$°C, Experiment 1MB.

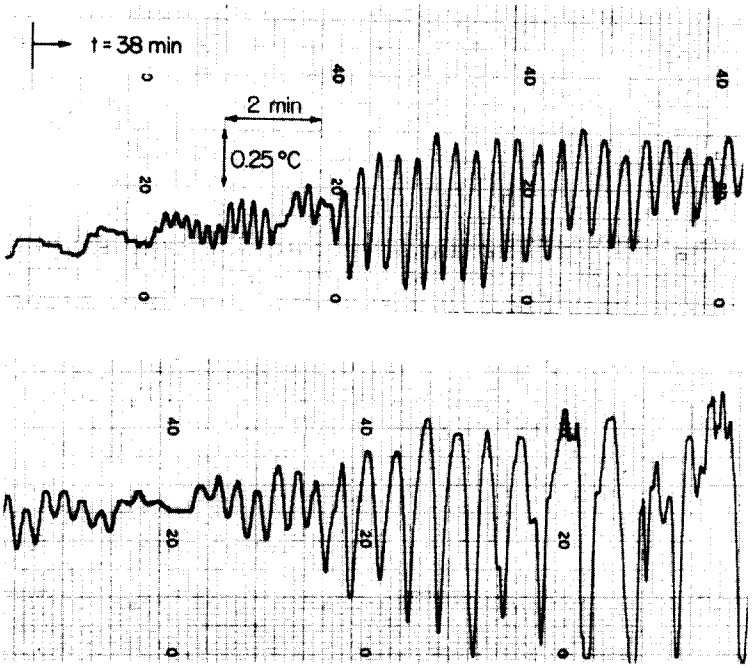

FIG. 5. Temperature fluctuations for the thermocouple located 5.56 mm above the bottom plate during melting from below, transition from laminar to turbulent flow, Experiment 1MB (bottom part of trace is continuation of top).

melting period the temperature shows no oscillations except for a linear rise until after a critical Rayleigh number has been exceeded. A regular oscillation of temperature (as shown on the LHS of Fig. 5) with an amplitude of about 0.075°C and period of 1.4 min was observed. The rate of average temperature rise was reduced significantly thereafter. The mechanisms causing these regular temperature oscillations are not clear. Verhoeven [15] observed a similar oscillation, but in a much longer period, in a vertical column of mercury heated from below in the absence of a phase change, and attributed the long period oscillation of temperature to the steady flow taking on a pulsed motion (pulsed flow). Whatever is the cause for flow, the oscillations of temperature must be due to the fluid motion driven by the buoyancy force. The constant amplitude and frequency of the temperature oscillations which appear to be unaffected by the changing aspect ratio of the liquid layer during melting imply that the flow pattern does not change and is steady at this stage.

At a certain critical melt depth or the corresponding Rayleigh number, the fluid layer becomes unstable and is readily subject to random disturbances. At this melting stage the oscillation frequency and amplitude of the temperature also increase. The temperature oscillates in a sinusoidal manner and is modulated with a very low frequency. The oscillations may be explained by the effect of generation of the disturbance and of stabilization by the viscous force. The disturbance may appear initially in the central region of the liquid-filled cavity and extend to the region near the wall. The first appearance of sinusoidal temperature oscillation in Experiment 7MB, during very late stages of melting, was found near the central region of the liquid layer. Also, in Experiment 6MB, the amplitude of the temperature oscillation near the central region of the liquid layer was found to be larger than near the wall region. The flow at this stage is in a transition regime. In fact, for a higher boundary temperature of melting (Experiments 2MB and 3MB) the flow in the steady and the transition period is so short that the temperature trace measurements do not provide a clear indication of these regimes and show a sudden occurrence of random fluctuations only after several cycles of oscillations [Fig. 6(a)].

At a critical Rayleigh number, the flow disturbance may become large enough to completely destroy the steady flow pattern. This disturbance has been indicated by the random fluctuations of temperature. The amplitude and frequency of the temperature oscillations are greatly increased [Fig. 6(a)]. There is a significant initial decrease and then an increase in the average temperature. This sequence may be due to the heated layer near the bottom plate being replaced by a cooled bulk fluid from the upper region. This cooled fluid is then heated or replaced by heated fluid nearby. The average temperature was steady later on, which implies that the bulk flow is also steady. At this stage the amplitude of the temperature fluctuations is larger than when the average temperature was varying and the flow is thought to be turbulent. Many spikes of temperature were observed similar to those found during the melting of paraffin [14]. However, the frequency of temperature

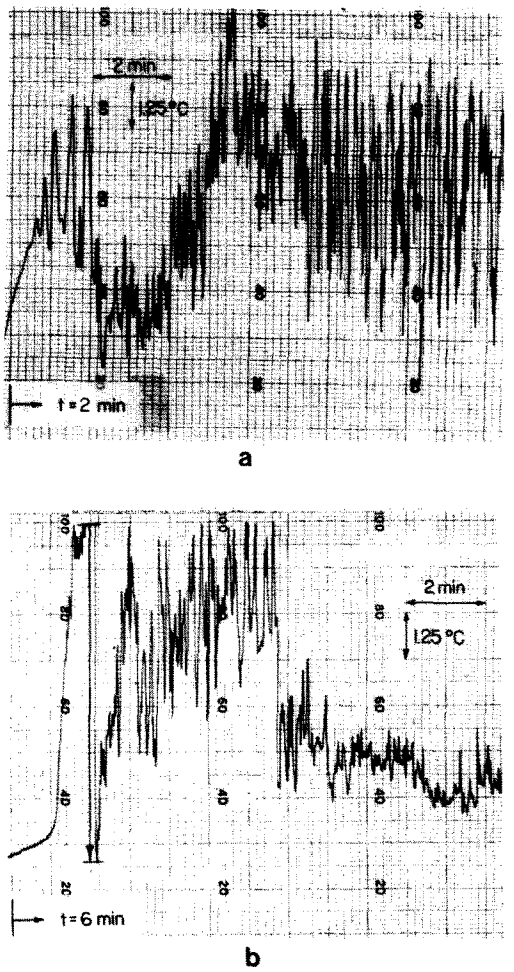

FIG. 6. Temperature fluctuations for Experiment 3MB $T_{wb} = 91.7°C$: (a) thermocouple located 4.76 mm above the bottom plate, (b) thermocouple located 24 mm above the bottom plate.

fluctuations appear to be higher in the metal system than in the paraffin system.

For the thermocouple located 24 mm above the bottom plate, the temperature started rising sharply in the conduction layer immediately after the melting front had passed over the sensor, and then oscillated once the sensor was in the convective layer of the thermal boundary layer. The flow at this melting stage is turbulent. The average temperature and the amplitude of its fluctuations increased until the edge of the thermal boundary layer was reached. As the melting front leaves the sensor the amplitude of the temperature fluctuations is gradually reduced. In the turbulent core region the amplitude of temperature fluctuation is generally small in comparison to those near the edge of the thermal boundary layer. The temperature fluctuations in the metal system are very similar to those in paraffin [14]. The temperature fluctuations measured by both thermocouples and the temperature distributions measured at later times were similar in the metal system and in the paraffin. This indicated that the flow structure in both systems was also similar. The heated (cooled) thermals were thought to be released from the thermal boundary layer adjacent to the bottom plate (solid–liquid interface) and dissipated by the viscous effects in the turbulent core. The fluid motion during melting in the metal system may be more intense than in the paraffin because of the higher frequency of the temperature fluctuation observed in the metal system.

Experiments with the same or very similar boundary conditions have been repeated, but the results obtained were not consistent. For example, in Experiment 7MB with $T_{wb} = 82.4°C$, the temperature fluctuation was not observed in the measurements of both thermocouples until $t = 62$ min. In Experiment 6MB [Fig. 7(a)] the temperature started oscillating 11 min after the initiation of melting. These oscillations of temperature seem to have been damped out before reappearing again in a periodic manner throughout the entire melting process. For the thermocouple located 24 mm above the bottom plate, the temperature did not show any oscillations until after about $t = 29$ min (or 18 min after the interface passed over the sensor). The amplitude of the oscillations was found to increase later and to be significantly larger than the amplitude near the bottom plate [Figs. 7(b) and (c)]. However, the random fluctuations of temperature were not observed and are believed to have been suppressed throughout the melting process.

Except for a smaller amplitude due to the suppression effect, the temperature fluctuations measured in Experiment 4MB at both locations are similar to those in Experiments 2MB and 3MB.

It was suspected that the composition stratification (segregation) might occur during the liquid metal settling in the test cell for steady state and during solidification from below before the initiation of the melting experiment. In fact, Lipowitz eutectic has four different components, and each has a different density. The constituents which have the largest density tend to settle at the bottom. Observations from the scanning electron microscope have shown that more tin (because it had the smallest density among the four) was found near the upper region than near the bottom region during the solidification experiments from above. Thus, the composition stratification during the melting and freezing process was thought to be the physical mechanism for suppressing the thermally-induced fluid motion.

4.2.3. *Comparison of predicted and measured interface positions.* Figure 8 shows a comparison of the measured and predicted solid–liquid interface positions for melting from below. A significant difference in the melting rates for the same or nearly the same bottom temperatures has been observed. This difference is attributed both to the unstable nature of flow and the inherent and uncontrollable composition stratification (segregation) of the material which suppresses the natural convection. These effects were not taken into account in the analysis. The melting rate at a higher bottom temperature may be lower than at a

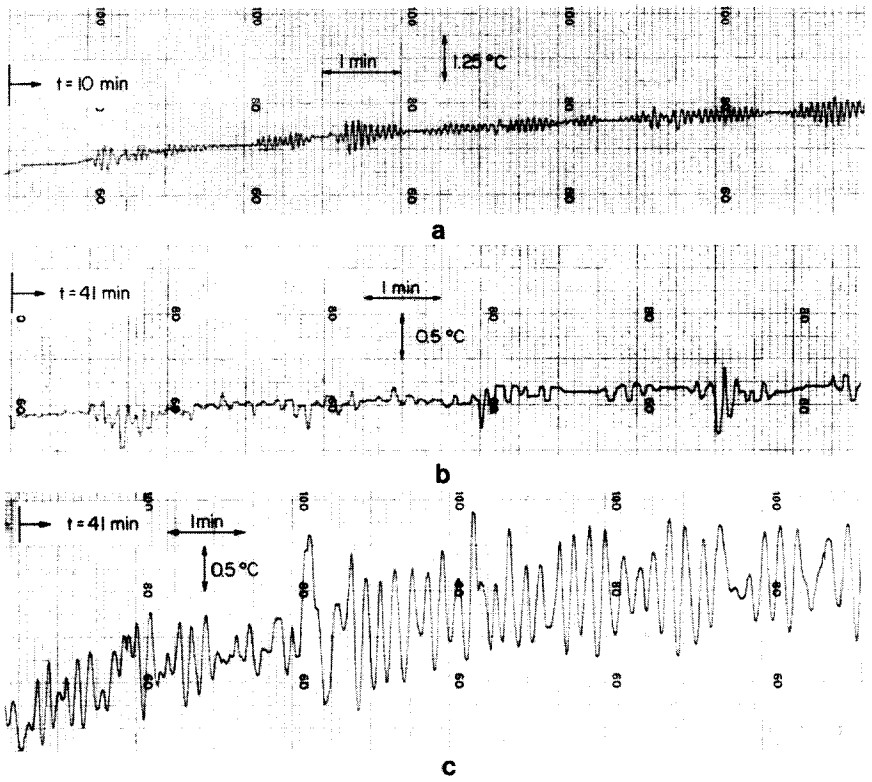

FIG. 7. Temperature fluctuations for Experiment 6MB, $T_{wb} = 89.7°C$: (a) thermocouple located 4.76 mm above the bottom plate, (b) at later times, (c) thermocouple located 24 mm above the bottom plate.

lower bottom temperature. The change in the melting temperature due to the composition stratification (Experiments 6MB and 7MB) is not significant. The melting rate with completely suppressed natural convection in the liquid still follows the predictions of the Neumann model (Fig. 8). The experimental data in Experiment 7MB were replotted in Fig. 3 for comparison with the data for melting from above. The agreement is very good until the very late melting stages when natural convection occurs. After this stage the melting rate continues to increase. In Experiments 2MB and 3MB, it may be that the composition stratification has the least effect so that the data follow the predicted trends well, but the melting rate in Experiment 4MB is slower due to the suppression of natural convection in the liquid. For Experiment 5MB, natural convection is suppressed initially and the data follow the Neumann model. Later, after purposely disturbing the suppression mechanism with the measuring probe in the liquid, the melting rate (velocity of the interface) is drastically increased and is close to that of Experiments 2MB and 3MB.

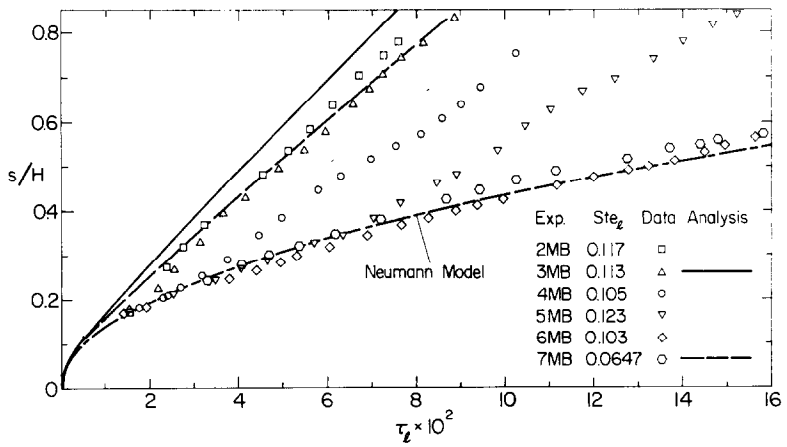

FIG. 8. Comparison of predicted and measured solid–liquid interface positions for melting from below.

4.3. *Freezing from above*

4.3.1. *Temperature fluctuation measurements.* The temperatures (Fig. 9) start fluctuating at both locations once the solidification process has been initiated. In the initial period, the average temperature measured near the central region shows a rapid decrease and then the average temperature near the bottom also decreases. This sequence is similar to the findings for the freezing of paraffin [14]. At the beginning the fluid becomes unstable locally and cooled parcels from the upper region flow downward, causing a rapid drop in temperature first near the central and then near the bottom region. The temperature near the bottom reaches a steady value rapidly while the one near the central region decreases further. The rate of its decrease depends on the intensity of the natural convection circulation (mixing). The average temperature decreases rapidly and then becomes steady when a higher intensity of natural convection mixing occurs [Fig. 9(b)]. The amplitude of the temperature fluctuations near the bottom is larger than near the central region and shows a slight increase after the average temperature becomes steady. The random fluctuations of temperature indicate that convection rolls or cells are not yet established in the liquid. However, because of the effect of the uncontrolled concentration stratification, for the same or for close boundary temperatures, a smaller amplitude and lower frequency of temperature fluctuation was observed in Experiment 4FA (Fig. 10). In some experiments with the same conditions, no fluctuations of temperature were observed, except during the initial period. The flow patterns are thus expected to be different for each experiment. However, the concentration gradient during the experiment of freezing from above may not always suppress the natural convection because of the temperature gradient.

4.3.2. *Comparison of predicted and measured interface positions.* A comparison of the measured and the predicted interface positions is shown in Fig. 11. The interface motion has been significantly affected by natural convection heat transfer in the liquid. The more intense the natural convection heat transfer in the liquid (as indicated by a larger amplitude and higher frequency of temperature fluctuations), the slower is the rate of freezing. Because of the uncontrolled effect of concentration stratification in the liquid which tends to

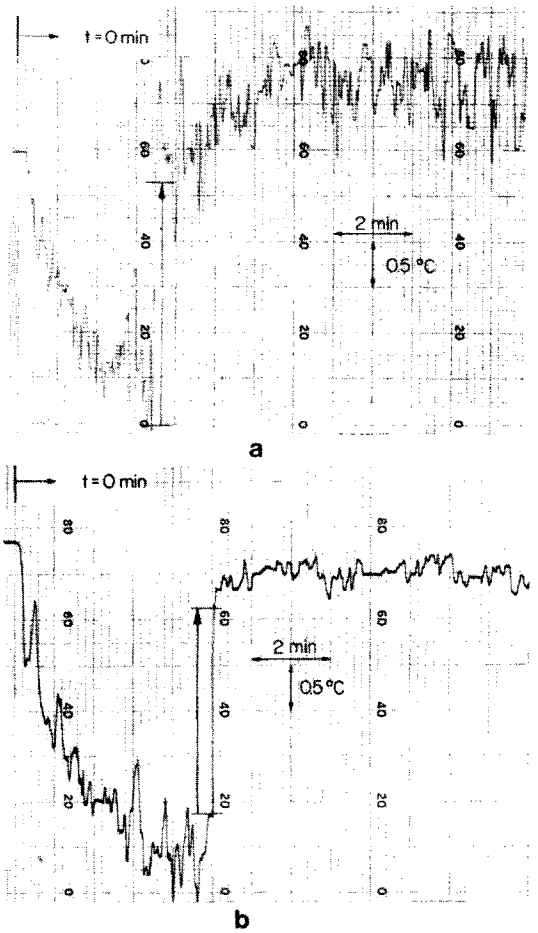

FIG. 9. Temperature fluctuations for Experiment 3FA, $T_{wt} = 57°C$, $T_{wb} = 76.1°C$: (a) thermocouple located 4.76 mm above the bottom plate, and (b) thermocouple located 24 mm above the bottom plate.

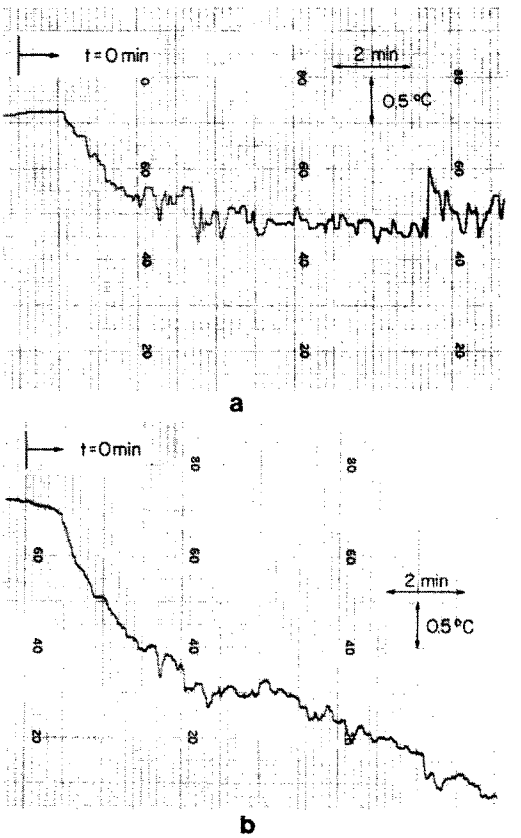

FIG. 10. Temperature fluctuations for Experiment 4FA, $T_{wt} = 56.7°C$, $T_{wb} = 75.9°C$: (a) thermocouple located 4.76 mm above the bottom plate, and (b) thermocouple located 24 mm above the bottom plate.

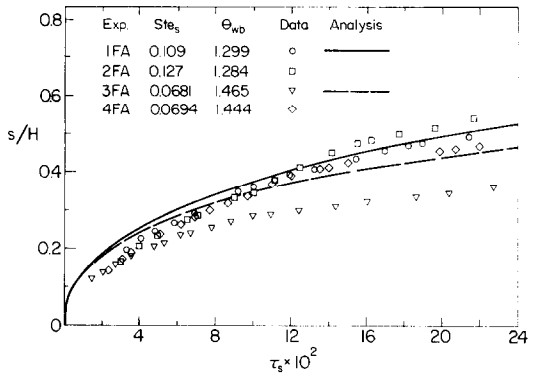

FIG. 11. Comparison of predicted and measured solid–liquid interface position for freezing from above.

suppress natural convection, different freezing rates for the same or close boundary temperatures have been obtained. For example, the experimental data resulting from the suppression of natural convection in Experiment 2FA are above the results and the predictions for Experiment 1FA. Thus, the suppression of the natural convection in the liquid increases the freezing rate. The experimental data of Experiment 1FA shows the best agreement with the prediction. The freezing rate in Experiment 3FA is significantly lower than that in Experiment 4FA and the prediction. From an examination of the temperature fluctuations we may conclude that the much slower solidification rate is attributed to augmentation of natural convection in the liquid. This may be due to the purposely mixing of the fluid prior to its having reached a uniform temperature and before the initiation of the solidification process. The fluid motion may have distributed the components in an unstable situation in such a way that once the solidification is initiated the concentration gradient may augment the natural convection.

5. CONCLUSIONS

The examination of the solid–liquid interface shape with the pour-out method during melting and freezing has provided evidence that the assumption of one-dimensional melting and freezing in a rectangular cavity is a reasonable one.

In the melting experiments from above and freezing from below, natural convection did not occur during the process of phase transformation. Heat conduction is the sole mode of energy transfer in the liquid. The measured interface positions agree with the predictions based on a pure conduction heat transfer model.

During the melting experiments from below, the temperature distribution and fluctuation measurements have provided information for indirectly deducing the flow structure. Different flow regimes have been obtained. Turbulent natural convection can significantly increase the melting rate. However, the inherent and uncontrolled composition stratification of the material before the initiation of melting was found to suppress natural convection and decrease the melting rate. The model predicted correctly the solid–liquid interface motion in the absence of compositional stratification.

During freezing experiments from below, the temperature fluctuation measurements also indicate suppression of natural convection. The freezing rate is higher when the suppression effect is large. In addition, natural convection was augmented due to the mixing of the fluid prior to the initiation of solidification, an action which can significantly retard the freezing rate. The model could not accurately predict the interface velocity under these conditions.

Acknowledgements—The work described in this paper was supported by the National Science Foundation Heat Transfer program under grant No. MEA-8014061.

REFERENCES

1. R. Viskanta, Phase change heat transfer, in *Solar Heat Storage: Latent Heat Materials* (edited by G. A. Lane). CRC Press, Boca Raton, Florida (1983).
2. N. W. Hale, Jr. and R. Viskanta, Solid–liquid phase-change heat transfer and interface motion in materials cooled or heated from above and below, *Int. J. Heat Mass Transfer* **23,** 283–292 (1980).
3. S. Ostrach, Fluid mechanics of crystal growth, The 1982 Freeman Scholar Lecture, November 1982 (to be published in *J. Fluid Engng*).
4. A. W. D. Hills, S. L. Malhotra and M. R. Moore, The solidification of pure metals (and eutectics) under unidirectional heat flow condition : II. Solidification in the presence of superheat, *Met. Trans.* **B6,** 131–142 (1975).
5. G. S. Cole and G. F. Bolling, Importance of natural convection in casting, *Trans. TMS-AIMS* **233,** 1568–1572 (1965).
6. K. Morizne, A. F. Witt and H. C. Gatos, Impurity distribution in single crystals, *J. Electrochem. Soc.* **114,** 738–742 (1976).
7. G. S. Cole and W. C. Winegard, Thermal convection during horizontal solidification of pure metals and alloys, *J. Inst. Metals* **93,** 153–164 (1964).
8. F. M. Chiesa and R. I. L. Guthie, Natural convection heat transfer rate during the solidification and melting of metals and alloy systems, *J. Heat Transfer* **99,** 520–526 (1977).
9. J. Szekely and P. S. Chhabra, The effect of natural convection on the shape and movement of the melt–solid interface in the controlled solidification, *Met. Trans.* **B1,** 1195–1203 (1970).
10. D. V. Hale, M. J. Hoover and M. J. O'Neill, *Phase Change Materials Handbook*, NASA CR-61363, NASA Contractor Report, Lockheed Missiles and Space Company, Huntsville, Alabama (1971).
11. K. G. Akhmetzyanov, V. E. Mikryukov and Ya. A. Turovskii, Some properties of the liquid alloy bismuth–cadmium–tin–lead, *Zuhr, Tekh. Fiz.* **20,** 203–216 (1950) (in Russian).
12. K. G. T. Hollands and G. D. Raithby, Natural convection, in *Handbook of Heat Transfer* (2nd edn.) (edited by W. M. Rohsenow *et al.*), McGraw-Hill, New York (1984) in press.
13. E. M. Sparrow, J. W. Ramsey and R. G. Kemink, Freezing controlled by natural convection, *J. Heat Transfer* **101,** 578–584 (1979).
14. R. Viskanta, C. J. Ho and C. Gau, Phase-change heat transfer in rectangular cavity, presented at the Fifth Miami International Conference on Alternative Energy Sources, 13–15 December 1982, Miami, Florida (to be published in the Proceedings of the Conference).
15. J. D. Verhoeven, Experimental study of thermal convection in a vertical cylinder of mercury heated from below, *Physics Fluids* **12,** 1733–1740 (1969).

FUSION ET SOLIDIFICATION D'UN SYSTEME METALLIQUE DANS UNE CAVITE RECTANGULAIRE

Résumé—On étudie le role de la convection naturelle sur le mouvement de l'interface solide–liquide pendant la fusion et la solidification du métal de Lipowitz dans une cavité rectangulaire. Les mesures des distributions de température et des fluctuations de température sont utilisées comme une indication qualitative des régimes d'écoulement de convection naturelle et des structures de fusion pendant le changement de phase. Les positions mesurées et calculées de l'interface pendant la solidification depuis le bas et le haut, aussi bien que pendant la fusion à partir du haut et du bas, montrent une correspondance raisonnablement bonne. La suppression de la convection naturelle dans le métal de Lipowitz, qui n'est pas prise en compte dans le modèle, conduit à une vitesse de fusion plus faible et à une plus grande vitesse de solidification que celles calculées.

SCHMELZEN UND ERSTARREN EINES METALLS IN EINEM RECHTWINKLIGEN HOHLRAUM

Zusammenfassung—Der Einfluß der freien Konvektion auf die Bewegung der Fest/Flüssig-Phasengrenze während des Schmelzens und Erstarrens eines Lipowitz-Metalls in einem rechteckigen Hohlraum wird untersucht. Die gemessenen Temperaturverteilungen einerseits und zeitlichen Temperaturverläufe andererseits werden als qualitativer Hinweis auf die Strömungszustände der freien Konvektion und die Strukturen der Schmelze während der Phasenänderung herangezogen. Die gemessenen und berechneten Verläufe der Fest/Flüssig-Phasengrenzfläche während des Erstarrens und Schmelzens an Ober- und Unterseite zeigen recht gute Übereinstimmung. Die Unterdrückung der freien Konvektion im Lipowitz-Metall, die im Modell nicht berücksichtigt wird, führt zu einer geringeren Schmelz- und höheren Erstarrungsgeschwindigkeit als vorausberechnet.

ПЛАВЛЕНИЕ И ЗАТВЕРДЕВАНИЕ МЕТАЛЛИЧЕСКОЙ СИСТЕМЫ В ПРЯМОУГОЛЬНОЙ ПОЛОСТИ

Аннотация—Исследуется роль естественной конвекции при движении границы раздела твердое тело-жидкость при плавлении и затвердевании металла в прямоугольной полости. Измерения как температурных распределений, так и температурных флуктуаций использовались для качественной идентификации режимов свободной конвекции и структур расплава при фазовом переходе. Получено довольно хорошее совпадение между измеренными и рассчитанными значениями положения границы раздела твердое тело-жидкость при затвердевании снизу и сверху и при плавлении сверху и снизу. Не учитывающееся в используемой модели подавление естественной конвекции в металле приводит к заниженному значению скорости плавления и к завышенной скорости затвердевания по сравнению с расчетными значениями.